

Charge-density-wave dynamics in TaS₃

A. Zettl and G. Grüner

Department of Physics, University of California at Los Angeles, Los Angeles, California 90024

(Received 1 October 1981)

We report the observation of strongly frequency (ω)-dependent conductivity (σ) in the charge-density-wave state of orthorhombic TaS₃. Both $\sigma(\omega)$ and the field-dependent conductivity $\sigma(E)$ are analyzed in terms of Bardeen's tunneling model. Experiments involving the joint application of ac and dc fields are also reported.

The linear chain compound TaS₃ (orthorhombic form) undergoes a Peierls transition¹ at temperature $T_p = 216$ K. The charge-density wave (CDW) is commensurate with the underlying lattice and has a periodicity $4c$, where c is the lattice constant along the chain direction.² We have reported earlier³ that the dc conductivity σ_{dc} is strongly nonlinear above a threshold electric field E_T and have also observed narrow band noise in the nonlinear region,⁴ with noise frequency $f_n \sim I_{CDW}$ where I_{CDW} is the current carried by the CDW. These observations, similar to those found in NbSe₃,⁵ give clear evidence that the nonlinear phenomena are associated with moving charge-density waves.

In this Communication we report the observation of frequency-dependent conductivity in the CDW state and also report on experiments involving a joint application of ac and dc driving fields. The frequency (ω) and electric field (E) dependent conductivity σ obeys the scaling relation proposed by Bardeen,⁶ with an additional contribution from the oscillating CDW at low frequencies.⁷ Excess dc conductivity can be induced by the application of an ac field, with ac-dc coupling characteristic of a strongly damped oscillator response.

The real and imaginary parts of the conductivity, $\text{Re}\sigma(\omega)$ and $\text{Im}\sigma(\omega)$, were measured using an HP 8754A network analyzer. The applied ac voltage amplitude V_{ac} was one to two orders of magnitude smaller than the threshold voltage V_T for the onset of dc nonlinearity. The experiments involving the joint application of ac and dc voltages were performed using radio-frequency circuits developed by us. The experiments were performed on needle-shaped crystals with the chain direction parallel to the needle axis. The measured σ then refers to the conductivity along the chain direction. In all cases two probe configurations were used, with contact resistances more than two orders of magnitude smaller than the sample resistance.

Figure 1 shows $\text{Re}\sigma(\omega)$ and $\text{Im}\sigma(\omega)$, normalized to the dc conductivity at room temperature, at various temperatures below $T_p = 216$ K. Down to about

130 K, $\text{Re}\sigma(\omega)$ smoothly increases from the dc value and saturates above 1 GHz; $\text{Im}\sigma(\omega)$ shows a maximum at frequencies where $\text{Re}\sigma(\omega)$ strongly increases with increasing ω . The overall behavior of both the real and imaginary parts is similar to that observed in NbSe₃ in both CDW states,^{7,8} and is characteristic of a strongly damped oscillator response. Following Lee, Rice, and Anderson⁹ the pinned CDW can be represented by a harmonic oscillator

$$\frac{d^2\phi}{dt^2} + \Gamma \frac{d\phi}{dt} + \omega_p^2 \phi = \frac{2k_{Fe}}{m + M_F} E(t), \quad (1)$$

where ϕ is the phase of the CDW. Γ is the damping

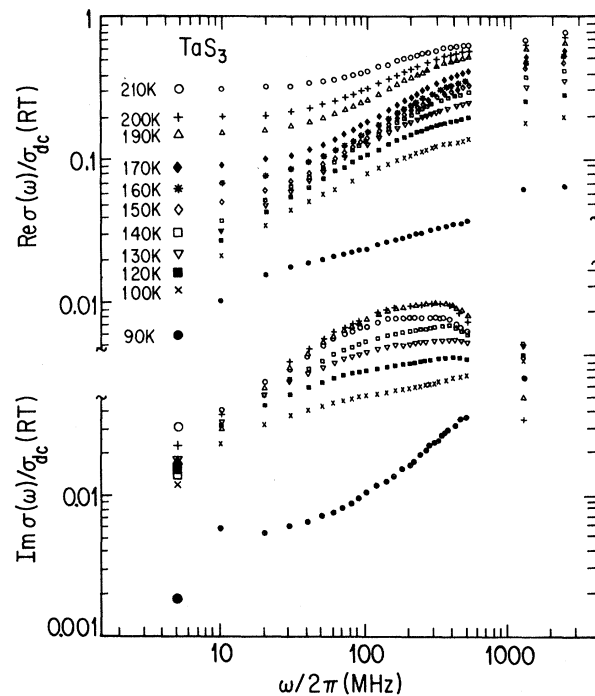


FIG. 1. $\text{Re}\sigma(\omega)$ and $\text{Im}\sigma(\omega)$, normalized to σ_{dc} measured at room temperature. The temperature is shown only for $\text{Re}\sigma(\omega)$; the same symbols are used for $\text{Im}\sigma(\omega)$.

constant and ω_p is the pinning frequency, and m and M_F are the band mass and Frölich mass, respectively. Equation (1) leads to the following conductivity when the inertia term is neglected:

$$\begin{aligned} \text{Re}\sigma(\omega) &= \frac{ne^2\Gamma}{m + M_F} \frac{\omega^2}{\omega^2 + (\omega_0^2/\Gamma)^2}, \\ \text{Im}\sigma(\omega) &= \frac{ne^2}{m + M_F\omega_p^2} \frac{\omega}{\omega^2 + (\omega_0^2/\Gamma)^2}. \end{aligned} \quad (2)$$

When the response is weakly damped, $\text{Re}\sigma(\omega)$ has a peak, and $\text{Im}\sigma(\omega)$ a zero crossing at $\omega = \omega_0^2/\Gamma$. Figure 1 then shows that the CDW response is not weakly damped, but rather overdamped. Fits of Eqs. (2) to the experimental data displayed in Fig. 1 give $\omega_{c0} = \omega_0^2/\Gamma = 240$ MHz, independent of temperature between T_p and 140 K. Below this temperature the $\sigma(\omega)$ curves become progressively broader, indicating a distribution of pinning energies, in accordance with the conclusion drawn from the nonlinear conductivity studies.^{3,10}

An alternative description of both $\sigma(\omega)$ and $\sigma(E)$, based on tunneling of macroscopic CDW segments, was proposed recently by Bardeen.⁶ The model leads to a CDW tunneling contribution to the dc conductivity

$$\sigma^t(E) = \begin{cases} 0 & (E < E_T) \\ \sigma^t(E \rightarrow \infty) \left[1 - \frac{E_T}{E} \right] \exp(-E_0/E) & (E \geq E_T) \end{cases}. \quad (3)$$

The parameter E_0 is given by $E_0 = \pi\epsilon_g^2/4\hbar e^*v_F$, where ϵ_g is the CDW gap and v_F the Fermi velocity, and $e^* = me/(m + M_F)$ is the effective charge of the CDW. The threshold field E_T is given by $e^*E_T L = \epsilon_g$, where L is the length of the CDW. The tunneling contribution to the ω -dependent conductivity is given by

$$\sigma^t(\omega/\omega_T) = \sigma_{dc}^t(E/E_T) \quad (4)$$

with the relation between the ω and E scale given by $\omega_T = e^*LE_T$. Thus the field- and the frequency-dependent conductivity have the same functional form. To test Eqs. (3) and (4) we have measured both $\sigma(E)$ and $\sigma(\omega)$ on the same sample during the same experimental run to avoid uncertainties associated with variations from sample to sample. Figure 2 shows $\sigma(\omega)$ and $\sigma(E)$ with $\sigma_{dc}(E \rightarrow 0)$ subtracted in both cases and with the ω and E scales adjusted at high frequencies and electric fields. The full line is Eq. (3) with chosen parameters $E_T = 1.3$ V/cm and $E_0 = 5E_T = 6.5$ V/cm. With the measured sample length $l = 0.4$ mm, this corresponds to a threshold voltage $V_T = E_T l = 52$ mV and $V_0 = E_0 l = 260$ mV. It is clear from Fig. 2 that $\sigma(E)$ is well described by Eq.

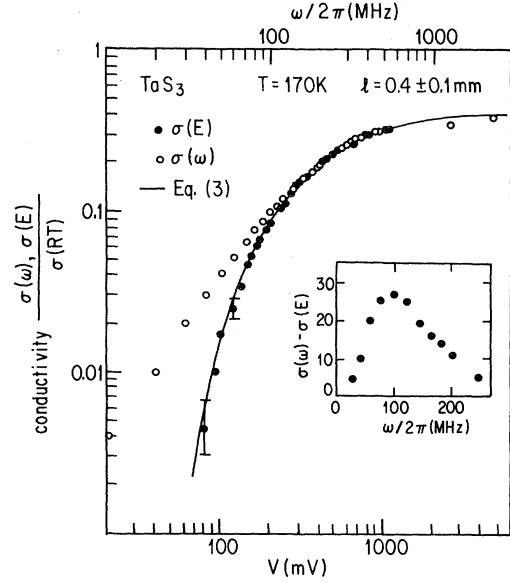


FIG. 2. Normalized $\sigma(E)$ and $\sigma(\omega)$ at $T = 170$ K. $\sigma_{dc}(E \rightarrow 0)$ has been subtracted in both cases. The solid curve is Eq. (3) with parameters $V_T = 52$ mV and $V_0 = 260$ mV. The ω and E scales are normalized using the measured values of σ above $3V_T$. The inset shows the difference between $\sigma(\omega)$ and $\sigma(E)$.

(3) over the whole electric field range. Also above about $E \sim 3E_T$, $\sigma(\omega)$ and $\sigma(E)$ have the same functional dependence on ω and E . The scaling relation, as shown in Fig. 2, gives a threshold frequency $\omega_T/2\pi = 25$ MHz. The CDW gap $\epsilon_g = \hbar\omega_T = 1.6 \times 10^{-19}$ ergs, orders of magnitude smaller than the thermal energy kT .

Below $E \sim 3E_T$, $\sigma(\omega) > \sigma(E)$, indicating an excess contribution to $\sigma(\omega)$. This has been suggested to reflect the excitation of oscillations of the pinned CDW.⁷ The pinned mode [Eq. (1)] leads to a conductivity contribution

$$\sigma^P(\omega) = \sigma^P(\omega_T) \frac{\Gamma^2\omega^2}{(\omega_T^2 - \omega^2) + \Gamma^2\omega^2}, \quad (5)$$

and the total ω -dependent conductivity is to first order given by

$$\sigma(\omega) = \sigma^t(\omega) + \sigma^P(\omega). \quad (6)$$

Making use of Eq. (4), $\sigma^P(\omega) = \sigma(\omega) - \sigma^t(E)$. This is shown in the inset of Fig. 2, where we have subtracted from $\sigma(\omega)$ the experimental field-dependent conductivity $\sigma(E)$. It is apparent that Eq. (5), with $\omega_T/2\pi \sim 100$ MHz and $\omega_T/\Gamma \sim 1$, provides an appropriate description of $\sigma^P(\omega)$. We conclude, therefore, that Bardeen's tunneling model accounts for both the field- and frequency-dependence conductivity in TaS₃. A similar analysis for NbSe₃ has been

performed recently,⁷ and similar conclusions concerning the field and frequency dependence of σ are obtained.

Next we discuss our experiments involving the joint application of ac and dc fields. For a conductivity which shows both a pronounced field and frequency dependence, various combinations of ac and dc fields $V = V_{dc} + V_{ac} \cos \omega t$ can be applied, and the dc and ac current and polarization can be detected to study the fine details of CDW transport. In this Communication we discuss two such experiments, which we believe give significant information about the CDW dynamics. We also give a tentative description, in terms of a classical analysis, for some of our findings.

1. *Search for photon-assisted tunneling.* The single-particle theory of tunnel junctions,¹¹ used to arrive at Eqs. (3) and (4), also predicts a finite dc current when the combined dc and ac field energy is larger than that corresponding to the threshold field, i.e., $eEL + \hbar\omega > eE_T L$. After establishing the relation between ω and E as shown in Fig. 2, we have tried to induce a dc current for various E and ω values which satisfy the condition for photon assisted tunneling. With a sensitivity two orders of magnitude larger than the theoretically predicted^{6,11} excess current I_{CDW} , we did not find an excess dc current and therefore conclude that photon-assisted tunneling does not occur for CDW transport.

2. *dc conductivity induced by large amplitude ac field.* While excess dc current cannot be observed by applying a high frequency but small amplitude ac field, dc current can be induced when $V_{dc} + V_{ac} > V_T$, i.e., by a large amplitude ac field. We have measured I_{dc} in the presence of an ac field of varying amplitude and frequency. Figure 3 shows the ac amplitude required to give a dc conductivity 1% or 2% higher than $\sigma_{dc}(V \rightarrow 0)$, at various frequencies, with parameters V_{dc} and V_T given on the figure. The strong increase of V_{ac} with increasing frequency has also been observed recently in NbSe₃.¹² For a strongly damped CDW the displacement cannot follow the ac field at higher frequencies; consequently, larger and larger ac amplitudes are required to lead to the same critical displacement for which dc conduction occurs. For an overdamped system, the assumption that a critical displacement X_{crit} is required for dc conduction leads

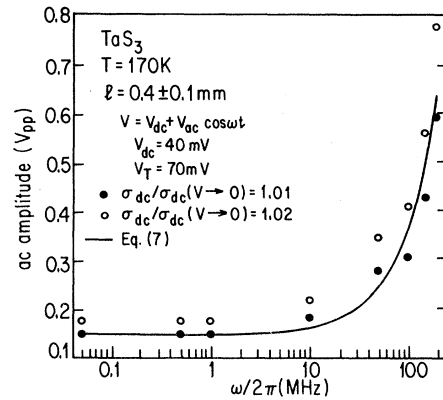


FIG. 3. Frequency dependence of the ac amplitude which leads to an excess dc conductivity 1% and 2% larger than the $\sigma(V \rightarrow 0)$ value. V_T refers to the threshold field for dc nonlinearity. The solid curve is Eq. (7) with parameters $V_{ac}(\omega=0) = 0.14$ V and $\omega_{c0}/2\pi = 50$ MHz.

to^{12,13}

$$E_{ac}(\omega) = E_{ac}(\omega=0) [1 - (\omega/\omega_{c0})^2]^{1/2}. \quad (7)$$

The full line of Fig. 3 is Eq. (7) with $V_{ac}(\omega=0) = 0.14$ V and $\omega_{c0}/2\pi = 50$ MHz.

In conclusion, we have tested experimentally the various aspects of CDW dynamics in TaS₃. We find that certain features, in particular, the detailed form of $\sigma(E)$ and the scaling relation of $\sigma(\omega)$ and $\sigma(E)$, strongly favor a description in terms of a quantum-mechanical tunneling of charge density waves.⁵ Photon-assisted tunneling, however, is not observed, and also a tentative explanation can be advanced, based on a classical motion,¹³ to account for our ac-dc coupling experiments. We believe that a microscopic theory of CDW transport should reflect both the quantum-mechanical and classical (time-dependent) aspects of our experimental findings.

Noted added in proof. The effect of ac excitation on the dc conductivity has also been interpreted in the framework of the tunneling model.¹⁴

We wish to thank A. H. Thompson for providing the samples, and J. Bardeen, W. G. Clark, and T. Holstein for useful discussions. This work was partially supported by the National Science Foundation Grant No. DMR-81-03085.

¹T. Sambongi, K. Tsutsumi, Y. Shiozaki, M. Yamamoto, K. Yamaya, and Y. Abe, *Solid State Commun.* **22**, 279 (1979).

²K. Tsutsumi, T. Sambongi, S. Kagoshima, and T. Ishiguro, *J. Phys. Soc. Jpn.* **44**, 1735 (1978).

³A. H. Thompson, A. Zettl, and G. Grüner, *Phys. Rev. Lett.* **47**, 64 (1981); A. Zettl, G. Grüner, and A. H. Thompson, *Solid State Commun.* **39**, 899 (1981).

⁴G. Grüner, A. Zettl, W. G. Clark, and A. H. Thompson, *Phys. Rev. B* **23**, 6813 (1981).

⁵R. M. Fleming and C. C. Grimes, *Phys. Rev. Lett.* **42**, 1423 (1979); R. M. Fleming, *Phys. Rev. B* **22**, 5606 (1980); P. Moneau, J. Richard, and M. Renard, *Phys. Rev. Lett.* **45**, 43 (1980); M. Weger, G. Grüner, and W. G. Clark, *Solid State Commun.* **35**, 243 (1980).

⁶J. Bardeen, *Phys. Rev. Lett.* **45**, 1978 (1980).

- ⁷G. Grüner, A. Zettl, W. G. Clark, and J. Bardeen, Phys. Rev. (in press).
- ⁸G. Grüner, L. C. Tippie, J. Sanny, W. G. Clark, and N. P. Ong, Phys. Rev. Lett. 45, 935 (1980).
- ⁹P. A. Lee, T. M. Rice, and P. W. Anderson, Solid State Commun. 14, 703 (1974).
- ¹⁰C. Jackson, A. Zettl, G. Grüner, and A. H. Thompson, Solid State Commun. 39, 531 (1981).
- ¹¹J. R. Tucker, IEEE J. Quant. Electron. 15, 1234 (1979).
- ¹²G. Grüner, W. G. Clark, and A. M. Portis, Phys. Rev. (in press).
- ¹³G. Grüner, A. Zawadowski, and P. M. Chaikin, Phys. Rev. Lett. 46, 511 (1981).
- ¹⁴J. R. Tucker, J. H. Miller, K. Seeger, and John Bardeen, Phys. Rev. B (in press).